0026-895X/93/040583-12$03.00/0

MOLECULAR PHARMACOLOGY, 43:583-594

Protein-Linked Receptors Labeled by [^{3}H]Histamine in Guinea Pig Cerebral Cortex. II. Mechanistic Basis for Multiple States of Affinity

WILLIAM G. SINKINS and JAMES W. WELLS

Faculty of Pharmacy, University of Toronto, Toronto, Ontario, Canada M5S 2S2

Received May 7, 1992; Accepted January 15, 1993

SUMMARY

Tritiated histamine labels multiple states of guanine nucleotide-binding protein-linked receptors in washed membranes from guinea pig cerebral cortex. The effects of guanylylimidodiphosphate identify the radioligand as an agonist, but the Hill coefficients can be as low as 0.78 for H_2 and H_3 agonists and 0.66 for antagonists. To examine the mechanistic basis of the binding patterns, the inhibitory behavior of 14 histaminergic ligands has been measured at 1.4 nM and 11 nM [^{3}H]histamine. In such experiments, the radioligand is both a second independent variable and an internal control; it is therefore possible to differentiate among mechanistic schemes for binding at equilibrium. When the data are analyzed in terms of distinct and independent sites, the relative capacities and the inferred affinities of [^{3}H]histamine differ significantly from ligand to ligand. Because the discrepancies persist for any degree of heterogeneity, the model can be rejected unequivocally. Several lines of evidence argue against the notion of a ligand-regulated equilibrium between two states of mutually independent sites. In particular, antagonists reveal a paradoxical arrangement in which the ligand appears to increase the relative number of sites in the state to which it binds more weakly; also, the Hill coefficients estimated at 1.4 nM [^{3}H]histamine are 1.54 for the H_2 agonist pyridylethylamine and 1.26 for the antagonist SK&F 93479 [*Mol. Pharmacol.* **43:** 569-582 (1993)]. High values of n_H suggest that one equivalent of bound ligand affects the affinity of the next, and a model based on cooperative interactions can predict most of the effects that are anomalous in the context of other schemes. H_2 agonists can be distinguished empirically from antagonists on the basis of their inhibitory behavior at two concentrations of [^{3}H]histamine. The trend includes two compounds that are H_2 agonists but H_3 antagonists, and the labeled sites therefore reveal an element of H_2 specificity.

Tritiated histamine labels a population of intriguing but pharmacologically elusive sites in membranes from guinea pig cortex (1). The noncompetitive effects of GMP-PNP identify the radioligand as an agonist and the sites as G protein-linked receptors. Elements of both H_2 and H_3 specificity emerge from the inhibitory behavior of 26 histaminergic ligands. Hill coefficients vary over an unexpectedly broad range, from 0.78 to 1.54 among agonists and from 0.66 to 1.26 among antagonists. In contrast, G protein-linked receptors generally appear homogeneous to antagonists ($n_H \approx 1$) (2); agonists discern heterogeneity when the radioligand is an antagonist ($n_H < 1$), but the sites appear homogeneous or nearly so to all compounds in assays with low concentrations of a radiolabeled agonist (e.g., Refs. 3 and 4). The low values of n_H obtained for some agonists and antagonists at the sites labeled by [^{3}H]histamine suggest that histaminergic receptors may reveal properties that are obscured in other systems. This possibility is supported by values of n_H greater than 1, which are difficult to explain in terms of the mechanistic schemes commonly used to rationalize the binding properties of G protein-linked receptors.

Histamine itself reveals two classes of sites when the data are described empirically as a sum of hyperbolic terms [i.e., $\sum_{j=1}^{n} F_j' K_j/(K_j + [L])$]; the sites of lower affinity account for about 10% of specific binding at the radioligand concentration used to assess the inhibitory effects of the unlabeled analogue (1). Two classes also are required for five agonists in addition to histamine and for six antagonists, but the contribution corresponding to the sites of lower affinity varies from 10% to 85% of specific binding. The differences are inconsistent with the notion of distinct and independent sites; rather, there appears to be a ligand-dependent interconversion from one state to the other. H_2 and H_3 agonists tend to favor the state of higher affinity; that is, the corresponding fraction of specific binding exceeds about 50% and correlates with the difference in the apparent affinity of the ligand for the two states [i.e., log (K_2/K_1)]. A similar pattern has been identified in the binding of agonists to β-adrenergic receptors (5, 6). H_2 and H_3 antago-

This investigation was supported by the Medical Research Council of Canada.

ABBREVIATIONS: GMP-PNP, guanylylimidodiphosphate; HEPES, *N*-(2-hydroxyethyl)piperazine-*N*'-ethanesulfonic acid; G protein, guanine nucleotide-binding protein.

nists reveal an analogous relationship between log (K_2/K_1) and the fraction of sites apparently in the state of low affinity. The behavior of antagonists implies a paradoxical arrangement in which the ligand promotes the state to which it binds more weakly; accordingly, the notion of a preference for one state or the other remains vague in mechanistic terms.

The binding patterns obtained for agonists at most G protein-linked receptors are inherently ambiguous. Data typically are acquired at a single concentration of the radioligand, and there is insufficient information to distinguish among mechanistic schemes that predict a dispersion of affinities for a system at equilibrium. It is widely recognized, for example, that the same rational function can describe a mixture of separate and intrinsically dissimilar sites on the one hand and a cooperative array on the other. Uncertainty over the mechanism of binding is partly responsible for uncertainty over the identity of the sites labeled by [^{3}H]histamine in guinea pig cortex. Pharmacological specificity has been defined in terms of a model that seems to be inappropriate, and the physical significance of the various parameters is therefore unclear.

The ambiguity typically associated with data acquired at equilibrium can be avoided by increasing the number of independent variables (7). In binding studies, a convenient and informative procedure is to characterize the inhibitory behavior of an unlabeled ligand at two or more concentrations of the radiolabeled probe. The data then can be analyzed in concert to distinguish between competing mechanistic proposals that otherwise are equivalent. This approach has been used to test the possibility that [^{3}H]histamine labels a heterogeneous population of distinct and independent sites, which is shown here to be inconsistent with the data. The results indicate that one ligand affects the binding of another in an apparently noncompetitive manner and suggest that the labeled sites can distinguish between H_2 agonists on the one hand and H_2 antagonists on the other. Among alternative schemes for the mechanism of binding, the data seem to favor models based on cooperative interactions between successive equivalents of ligand over models involving a ligand-regulated equilibrium between free and G protein-coupled receptors. The results of the present investigation are of general relevance to questions regarding the mechanisms of binding and transduction in G protein-mediated systems; the approach is broadly applicable to the mechanistic interpretation of binding data acquired at equilibrium.

Materials and Methods

[^{3}H]Histamine was obtained either from Amersham Corporation (33–54 Ci/mmol) or from New England Nuclear (32.1–48.1 Ci/mmol); [^{3}H]tiotidine (83.6 Ci/mmol) was obtained from New England Nuclear. Experimental procedures and other details are described in the preceding paper (1). Binding was measured in homogenates of EDTA-washed membranes prepared from the cerebral cortices of male Hartley guinea pigs. The buffer solution contained 50 mM HEPES, 100 mM NaCl, 10 mM $MgCl_2$, and 1.0 mM EDTA, pH 7.48. The reaction mixture was equilibrated for 4 hr at 30°, and bound radioligand was then separated on fiberglass filters. Most experiments involved parallel assays with two concentrations of [^{3}H]histamine (1.29–1.47 nM and 10.14–11.87 nM) and graded concentrations of an unlabeled ligand; binding at each concentration of the radioligand also was measured in the presence of 1.0 mM unlabeled histamine. Data were analyzed according to the procedures described in the accompanying paper (1), and equations are numbered accordingly. For each experiment, an estimate of binding in the absence of unlabeled ligand was included in the analysis; that in the presence of 1.0 mM unlabeled histamine was omitted but is shown in each figure for the purpose of comparison.

Data from replicated experiments have been presented with reference to a single fitted curve in Figs. 1–3, which illustrate the results of simultaneous analyses in terms of distinct and independent sites (i.e., scheme 2 and eq. 4 in Ref. 1). To obtain the values plotted on the ordinate, estimates of B_{obsd} were adjusted as follows:

$$B'_{obsd} = B_{obsd} \frac{f(\bar{\mathbf{x}}_i, \bar{\mathbf{a}})}{f(\mathbf{x}_i, \mathbf{a})}$$

The function f represents eq. 4. The vectors $\mathbf{x}_i$ and $\mathbf{a}$ represent the independent variables at point i and the fitted parameters for the set of data under consideration; $\bar{\mathbf{x}}_i$ and $\bar{\mathbf{a}}$ are the corresponding vectors in which values that differ from experiment to experiment have been replaced by the means for all experiments included in the analysis. Values of B'_{obsd} at the same $\mathbf{x}_i$ are presented as the mean; the standard errors generally are within the diameter of the symbols, as illustrated in Fig. 3.

Results

Binding in the absence and presence of GMP-PNP was characterized by isotopic dilution of 1.4 nM and 11 nM [^{3}H] histamine (Fig. 1). Measurements at the two concentrations of the radioligand were made concomitantly using membranes from the same homogenate; those with and without the nucleotide were made in separate experiments. The data were analyzed in terms of the multisite model represented by scheme 2 and eq. 4 in the accompanying paper (1). Each experiment was

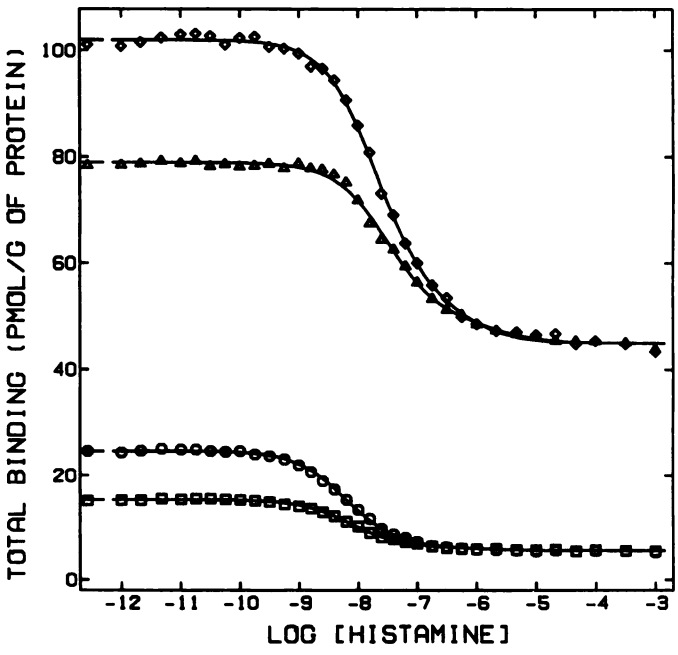

Fig. 1. Effect of GMP-PNP and [^{3}H]histamine on inhibition by unlabeled histamine. Total binding was measured after incubation of the membranes with the radioligand (○, □, 1.38–1.42 nM; ◇, △, 11.04–11.57 nM) plus unlabeled histamine in the absence of guanyl nucleotide (○, ◇) and in the presence of 0.1 mM GMP-PNP (□, △). The data are from four experiments, each of which included assays at both concentrations of the radioligand; GMP-PNP was added in two experiments. The *lines* represent the best fits of eq. 4 (n = 2) to the two sets of data acquired under the same conditions, and the parametric values are listed in Table 1A. Individual *points* represent the mean values of B'_{obsd} obtained as described in Materials and Methods; *those at the lower end of the abscissa* represent binding in the absence of unlabeled histamine.

performed twice, and the two sets of data acquired under the same conditions were assigned single values of K_{P_j} and F_j. Two classes of sites were required to achieve a satisfactory fit either with or without the nucleotide ($p_2 < 0.00001$); the fitted curves are illustrated in Fig. 1, and the parametric values are listed in Table 1A.

If the binding patterns denote distinct and independent sites (i.e., scheme 2 in Ref. 1), the fitted estimates of K_{P_j} and F_j ought to be independent of the concentration of the radioligand. In contrast, the results listed in Table 1A indicate that a 7.9-fold increase in the concentration of [^{3}H]histamine is accompanied by a 3–4-fold increase in K_{P_1} and a 10–20-fold increase in K_{P_2}; capacity is increased at both classes of sites, with a proportionally larger change in $R_{2,t}$. The discrepancies were tested for significance by assigning single values of all parameters to data acquired at both concentrations of the radioligand. Such forced compliance with scheme 2 causes a 1.7–2.1-fold increase in the weighted sum of squares ($p < 0.00001$; Table 1B), and the fitted curves deviate appreciably from the data. The disagreement is not resolved if the analysis is repeated with three classes of sites rather than two. The inability of eq. 4 to describe the data suggests that scheme 2 is inappropriate. Because the model is in effect empirical, the physical significance of all parameters is unclear.

Discrepancies among the parametric values estimated according to eq. 4 reflect inconsistencies in the concentration-dependent effects of labeled and unlabeled histamine. It follows that the problem may arise from an error in the specific activity of the radioligand (SA), which was taken as that stated by the manufacturer. This possibility was tested by means of an additional parameter that permitted the values of SA and $[P]_t$ to be adjusted for any error in SA. The same lot of [^{3}H] histamine was used for all of the assays represented in Table 1, and a single correction is therefore sufficient. With data acquired at one concentration of the radioligand, the added factor is redundant and undefined; with data acquired at both concentrations, a well defined estimate is obtained when other parameters are assigned as in the analyses of Table 1B. The fitted values are 0.85 ± 0.02 and 0.82 ± 0.04 in the absence and presence of GMP-PNP, respectively, which suggests that the true specific activity was about 84% of the published value if scheme 2 is indeed the correct model. Scheme 2 remains unacceptable, however, because the additional parameter is unable to eliminate the discrepancies in K_{P_j}, F_2, and $[R]_t$; for data acquired either with or without the nucleotide, the reduced sum of squares from the combined fit (see Table 1B) remains significantly greater than that from the independent fits represented in Table 1A ($p < 0.00001$). The failure of the model thus cannot be attributed to an error in the specific activity of [^{3}H]histamine.

The inadmissibility of scheme 2 can be demonstrated empirically by means of eq. 3 ($n = 2$), which is formally equivalent to eq. 4 but does not include the concentration of [^{3}H]histamine. The values of F'_2 listed in Table 1A indicate that a 7.9-fold increase in the concentration of the radioligand has little or no effect on the fraction of specific binding corresponding to the sites of lower affinity. In contrast, eq. 4 predicts that F'_2 will increase with the concentration of the radioligand, asymptotically approaching F_2 as the radioligand becomes saturating and the Hill coefficient approaches 1. An estimate of the increase expected with the present data is given in Table 1B, where values of F'_2 correspond to the best compromise that can be obtained with eq. 4.

Eight H_2 agonists and five H_2 antagonists were used to examine the effects of other compounds on the binding of [^{3}H] histamine. The inhibitory behavior of each was measured in two to four experiments conducted at 1.4 nM and 11 nM [^{3}H] histamine, and the pooled data were analyzed according to eq. 4 with single values of K_{P_j}, K_{A_j}, and F_j. All compounds revealed at least two classes of sites; the parametric values are listed in Table 2, and the fitted curves are illustrated in Figs. 2 and 3. In each case, the apparent heterogeneity was recognized both by [^{3}H]histamine and by the unlabeled ligand; the weighted sum of squares is significantly higher with single rather than separate values of either K_{P_j} (i.e., $K_{P_1} = K_{P_2}$, $K_{A_1} \neq K_{A_2}$) or K_{A_j} (i.e., $K_{P_1} \neq K_{P_2}$, $K_{A_1} = K_{A_2}$) for sites of either class ($p < 0.00001$).

The values of K_{A_1}, K_{A_2}, and K_{P_1} are well defined for most compounds, as indicated by relatively low error (Table 2) and

TABLE 1

Effect of GMP-PNP and the radioligand on the binding of histamine in terms of scheme 2

Data from duplicate experiments at graded concentrations of unlabeled histamine were analyzed simultaneously according to eq. 4 ($n = 2$); the concentrations of GMP-PNP and [^{3}H]histamine were as shown in the table. Parametric values were assigned as follows. A, Single values of K_{P_1}, K_{P_2}, and F_2 were common to the two sets of data acquired under the same conditions; values of $[R]_t$ and NS were assigned individually to each set of data. B, Single values of K_{P_1}, K_{P_2}, and F_2 were common to all data acquired in the absence of GMP-PNP on the one hand and in the presence of GMP-PNP on the other; single values of $[R]_t$ and NS were common to the two sets of data acquired at 1.4 nM and 11 nM [^{3}H]histamine in the same experiment, and separate values were assigned to the data from different experiments. Fitted estimates of $[R]_t$ were normalized per g of protein to obtain R_t; $R_{1,t}$ and $R_{2,t}$ were calculated in turn from R_t and F_2, and the two values of each were averaged to obtain the means ± standard errors listed in the table. The data and fitted curves are illustrated in Fig. 1, and further details are described in the text.

Analysis	GMP-PNP	[^{3}H]Histamine	Eq. 4 ($n = 2$)							Eq. 3, F'_2[b]
			p[a]	log K_{P_1}	log K_{P_2}	F_2	$R_{1,t}$	$R_{2,t}$	R_t	
	mM	nM					pmol/g	pmol/g	pmol/g	
A	0	1.4	0.15	−8.47 ± 0.04	−7.35 ± 0.16	0.61 ± 0.03	58 ± 5	89 ± 7	147 ± 12	0.14
	0	11	0.81	−8.03 ± 0.05	−6.10 ± 0.17	0.84 ± 0.03	91 ± 8	475 ± 42	566 ± 50	0.12
	0.1	1.4	0.21	−8.30 ± 0.03	−6.75 ± 0.20	0.77 ± 0.05	41 ± 1	135 ± 2	176 ± 2	0.10
	0.1	11	0.39	−7.72 ± 0.05	−5.65 ± 0.22	0.92 ± 0.03	82 ± 1	936 ± 2	1018 ± 2	0.13
B	0	1.4	<0.00001	−8.55 ± 0.02	−6.79 ± 0.08	0.82 ± 0.01	52 ± 4	236 ± 20	288 ± 24	
	0	11								0.27
	0.1	1.4	<0.00001	−8.52 ± 0.04	−6.80 ± 0.07	0.90 ± 0.01	26 ± 1	220 ± 2	246 ± 2	0.19
	0.1	11								0.42

[a] Level of confidence for the increase in the sum of squares with single rather than separate values of K_{P_1}, K_{P_2}, and F_2 for the two sets of data in each analysis (A) and over that from the corresponding analyses in A (B).

[b] Values of F'_2 listed in the table are inferred in terms of eq. 3 ($n = 2$) from best fits of eq. 4. The values obtained from best fits of eq. 3 to the data *per se* are similar to those in A.

TABLE 2

Binding of agonists and antagonists at two concentrations of [^{3}H]histamine

Eq. 4 (n = 2) was fitted to the combined data acquired at two concentrations of [^{3}H]histamine (1.29–1.47 nM and 10.14–11.87 nM) in each of two to four experiments with each ligand; the number of experiments represented in each analysis is shown in parentheses. Single values of K_{A_1}, K_{P_1}, and F_2 were common to all of the data, and the results are listed in the table; single values of $[R]_t$ and *NS* were common to the data acquired at both concentrations of the radioligand in the same experiment. The data and fitted curves for 11 of the compounds are illustrated in Figs. 2 and 3.

Ligand	log K_{A_1}	log K_{A_2}	log K_{P_1}	log K_{P_2}	F_2	K_{A_2}/K_{A_1}	K_{P_2}/K_{P_1}	$R_{2,t}/K_{P_2}$[a]	Relative ΔB[b]	$IC_{50(1.1)}/IC_{50(1.4)}$[c]
H_2 agonists										
Histamine[d,e]	[e]	[e]	−8.45 ± 0.02	−6.34 ± 0.22	0.91 ± 0.04					
(*R*)-(−)-Sopromidine[f] (8)	−7.7166 ± 0.0011	−3.3522 ± 0.0177	−8.37 ± 0.01	−5.60 ± 1.81	0.94 ± 0.23	4500	590	5.4	0.96, 0.98	3.1
N^g-Methylhistamine (2)	−9.2277 ± 0.0088	−6.5555 ± 0.0100	−8.54 ± 0.03	−5.13 ± 1.33	0.98 ± 0.05	525	2600	11	1.00, 0.93	4.2
Norclobenpit (2)	−5.9999 ± 0.0022	−3.9966 ± 0.0053	−8.45 ± 0.01	−7.98 ± 0.15	0.14 ± 0.03	110	3.0	12	1.08, 1.00	2.8
Dimaprit (8)	−6.5165 ± 0.0044	−4.4188 ± 0.0398	−8.41 ± 0.03	−6.12 ± 3.60	0.89 ± 0.84	95	195	8.0	0.97, 0.94	3.3
4-Methylhistamine (8)	−5.5422 ± 0.0033	−3.8811 ± 0.0311	−8.42 ± 0.02	−7.22 ± 0.04	0.38 ± 0.19	41	16	8.0	1.01, 0.99	3.0
Imidazolylpropylguanidine[f] (2)	−9.0066 ± 0.0392	−7.6611 ± 0.0033	−9.43 ± 0.32	−6.49 ± 1.16	0.98 ± 0.04	28	870	37	0.98, 0.93	4.4
N^g,*N*^{g}-Dimethylhistamine (8)	−8.8422 ± 0.0111	−7.7255 ± 0.0168	−8.66 ± 0.11	−7.43 ± 0.28	0.72 ± 0.10	15	17	31	1.04, 1.03	3.8
Impromidine (8)	−6.6733 ± 0.0044	−7.7377 ± 0.0066	−8.60 ± 0.02	−7.92 ± 0.11	0.52 ± 0.04	0.23	4.8	43	1.04, 0.98	1.9
H_2 antagonists										
SK&F 92594[h] (8)	−4.4771 ± 0.0094	−5.5700 ± 0.0088	−8.29 ± 0.03	−7.75 ± 0.12	0.54 ± 0.05	0.10	3.5	31	0.61, 0.80	1.4
(*S*)-(+)-Sopromidine (4)	−5.5659 ± 0.0199	−6.6755 ± 0.0086	−8.59 ± 0.01	−8.14 ± 0.05	0.83 ± 0.05	0.087	2.8	170	1.27, 1.45	1.5
Burimamide (2)	−6.6844 ± 0.0122	−8.3283 ± 0.0166	−8.66 ± 0.06	−8.33 ± 0.11	0.52 ± 0.06	0.036	2.1	77	0.96, 0.91	1.6
Norburimamide (4)	−5.5988 ± 0.0022	−8.6038 ± 0.0059	−8.38 ± 0.01	−8.00 ± 0.08	0.26 ± 0.02	0.0089	2.4	25	1.02, 1.04	2.0
SK&F 92374[h] (8)	−5.5765 ± 0.0022	−8.8366 ± 0.0338	−8.49 ± 0.01	−6.07 ± 2.41	0.93 ± 0.39	0.0025	260	11	1.06, 1.01	2.2

[a] The fitted estimates of F_2 and $[R]_t$ were used to calculate $[R_2]_t$ and the corresponding value of $R_{2,t}$ (pmol/g of protein) for each experiment; the mean from two to four experiments is shown relative to K_{P_2}.

[b] Individual sets of data within each experiment were analyzed according to eq. 3 (n = 2) to obtain the quantity $B_{A=0}-B_{A=\infty}$ (ΔB), in units of pmol/g of protein; the mean values of ΔB from two to four experiments with each ligand then were averaged to obtain the means for all ligands (22.06 ± 0.09 pmol/g of protein with 1.4 nM [^{3}H]histamine and 64 ± 3 pmol/g of protein with 11 nM [^{3}H]histamine). Values listed in the table represent the means for individual ligands relative to the overall means for binding at 1.44 nM and 11 nM [^{3}H]histamine.

[c] IC_{50} represents the concentration of unlabeled ligand that reduces specific binding by 50% at each concentration of [^{3}H]histamine, as defined by the fitted curves illustrated in Figs. 2 and 3 (eq. 4, n = 2).

[d] Eq. 4 (n = 2) was fitted to the data from eight experiments performed with graded concentrations of labeled and unlabeled histamine. Further details are given in the legend to Table 2D of the preceding paper (1).

[e] K_{A_1} is assumed to equal K_{P_1} in the derivation of the polynomial used to calculate $[P]_b$ for eq. 4.

[f] (*R*)-(−)-Sopromidine and imidazolylpropylguanidine are agonists at H_2 receptors but antagonists at H_3 receptors (1).

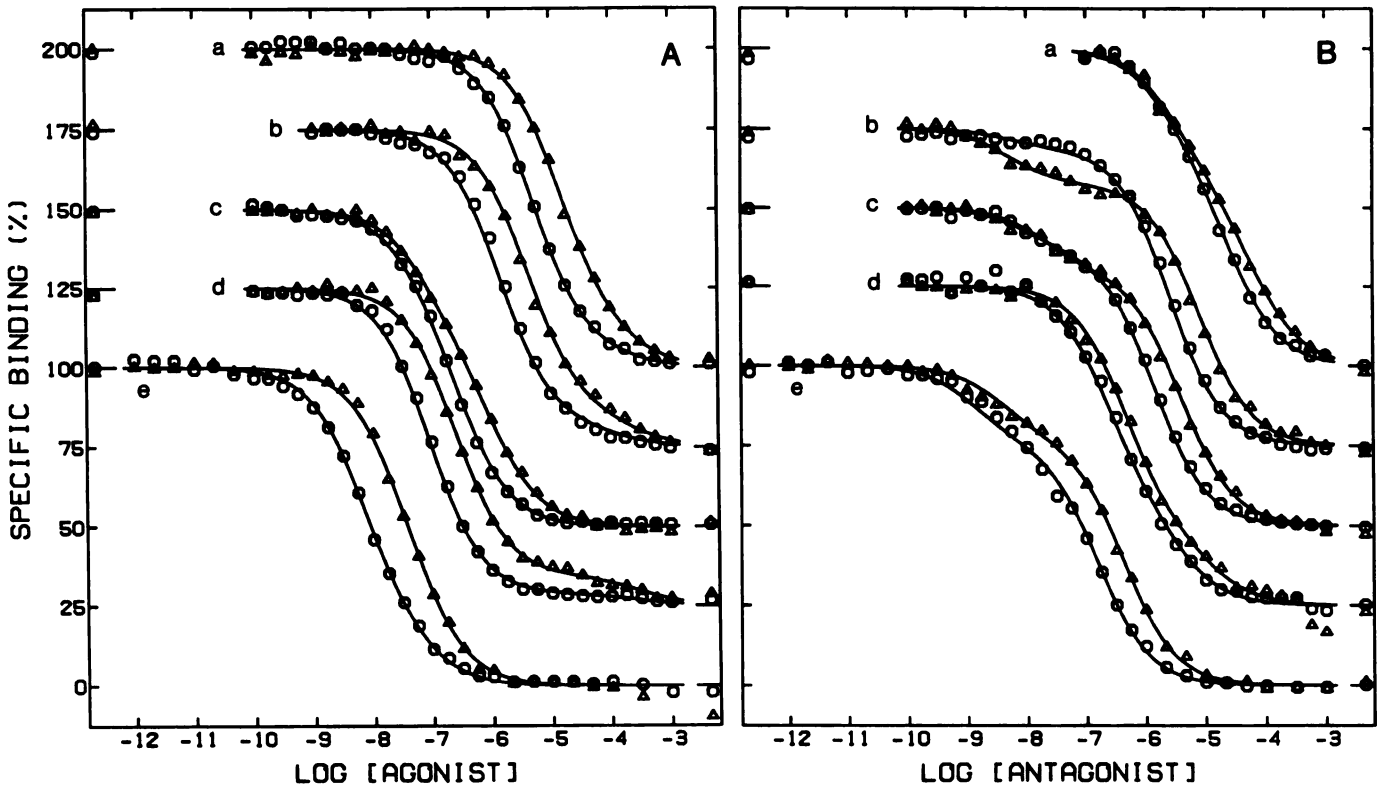

Fig. 2. Inhibition of [^{3}H]histamine by agonists and antagonists at two concentrations of the radioligand. Total binding was measured after incubation of the membranes with [^{3}H]histamine (○, 1.29–1.47 nM; △, 10.14–11.87 nM) and either an agonist (A) or an antagonist (B) at the concentrations shown on the *abscissa*. The *lines* represent best fits of eq. 4 (n = 2) to the combined data acquired at both concentrations of the radioligand in two to four experiments with each ligand; the parametric values and further details regarding the analyses are given in Table 2. Individual *points* represent the mean values of B'_{obsd} obtained as described in Materials and Methods. *Values plotted on the ordinate* have been normalized to the fitted asymptotes taken as 100 and 0, and the *curves* for successive ligands have been offset by 25% for clarity. *Points at the lower end of the abscissa* represent binding in the absence of unlabeled ligand; *those at the upper end* represent binding in the presence of 1.0 mM histamine and were excluded from the analyses. Individual compounds are as follows: A, *a*, 4-methylhistamine; *b*, nordimaprit; *c*, impromidine; *d*, (*R*)-(−)-sopromidine; *e*, N^{α},N^{α}-dimethylhistamine; B, *a*, SK&F 92540; *b*, SK&F 92374; *c*, norburimamide; *d*, (*S*)-(+)-sopromidine; *e*, burimamide.

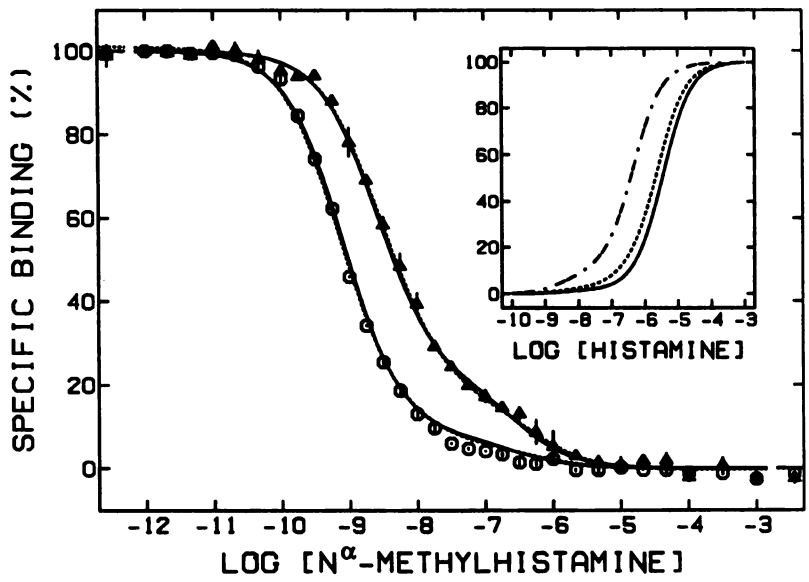

Fig. 3. Inhibition of [^{3}H]histamine by N^{α}-methylhistamine at two concentrations of the radioligand. Total binding was measured after incubation of the membranes with [^{3}H]histamine (○, 1.33–1.36 nM; △, 11.06–11.07 nM) and N^{α}-methylhistamine at the concentrations shown on the *abscissa*. *Main panel*, the *lines* represent the best fit of eq. 4 to the combined data from two experiments (——, n = 2; - - -, n = 3). The parametric values obtained for two classes of sites are listed in Table 2; those for three classes of sites are as follows: log K_{A_1} = −9.38 ± 0.28, log K_{A_2} = −7.94 ± 0.83, log K_{A_3} = −6.25 ± 0.19, log K_{P_1} = −8.64 ± 0.20, log K_{P_2} = −6.91 ± 1.84, log K_{P_3} = −5.61 ± 1.79, F_2 = 0.05 ± 0.22, and F_3 = 0.93 ± 0.30. *Values plotted on the ordinate* were normalized to the fitted asymptotes for n = 2 taken as 100 and 0. Further details are given in the legends to Table 2 and Fig. 2. *Inset*, the *rightmost curves* were calculated from the values of K_{P_j} and F_j obtained from the data shown in the figure and represent the binding of histamine as inferred from the inhibitory behavior of N^{α}-methylhistamine (——, n = 2; - - -, n = 3). The *leftmost curve* was calculated from the parametric values listed in Table 2 for the binding of histamine alone (— · — · — ·).

a low degree of correlation with other parameters. In contrast, K_{P_2} is characterized by larger errors and is highly correlated with F_2 and $[R]_t$; this uncertainty arises in part from the long extrapolation associated with the low occupancy achieved by 11 nM [^{3}H]histamine at the sites of lower affinity for the radioligand (i.e., [P] < K_{P_2}). The value of K_{P_2} nevertheless is associated with a minimum in the sum of squares, as illustrated by the map obtained for the agonist N^{α}-methylhistamine (Fig. 4); at a confidence level of 95%, the upper and lower limits on log K_{P_2} are −3.67 and −6.56, respectively. Bounded estimates of K_{P_2} are a consequence of experimental design and the attendant constraints that can be placed on $[R]_t$ and NS during the fitting procedure. With each ligand, assays at 1.4 and 11 nM [^{3}H]histamine were performed concomitantly on aliquots

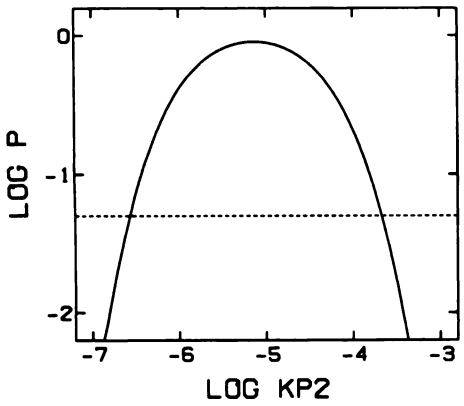

Fig. 4. Effect of K_{P_2} on goodness of fit for N^{α}-methylhistamine. Eq. 4 (n = 2) was fitted to the combined data obtained from two experiments with N^{α}-methylhistamine and represented in Fig. 3. Single values of K_{P_j}, K_{A_j}, and F_2 were common to all of the data; $[R]_t$ and NS were common to data from the same experiment. The effect of K_{P_2} was mapped in a series of analyses in which log K_{P_2} was fixed at different values over the range shown on the *abscissa*. The global sum of squares from each fit was compared with that from the best fit to obtain the F statistic and the corresponding value of log p plotted on the *ordinate*. - - -, 95% level of confidence.

from the same preparation of membranes; accordingly, single values of both parameters can be assigned to the data acquired at both concentrations of the radioligand. A relationship is thereby established between absolute levels of specific binding and the position of the curve on the abscissa. Without the constraint in $[R]_t$, only a lower limit can be placed on the value of K_{P_2}.

As illustrated in Fig. 2, there generally is good agreement between the fitted curves obtained with two classes of sites and the pooled data acquired at both concentrations of [^{3}H]histamine. Seven of the 13 compounds show a somewhat better fit with three classes of sites, as indicated by the sum of squares, but the various parameters are highly correlated; a unique solution generally requires constraints on one or more of K_{P_j}, K_{A_j}, and F_j, and the improvement is small in absolute terms. The difference between two and three classes of sites is illustrated in Fig. 3, where the fitted curves are compared for the agonist N^{α}-methylhistamine (p = 0.0045). There is little net effect on the inferred binding of histamine calculated from the values of K_{P_j} and F_j (Fig. 3, *inset*). No further improvement is obtained with four classes of sites rather than three ($p > 0.1$).

Agreement between the data and scheme 2 can be found for most compounds but not all, and the most striking exception is N^{α}-methylhistamine. For any value of n, eq. 4 yields relatively large deviations between the fitted curves and data acquired at the lower concentration of [^{3}H]histamine. As illustrated in Fig. 3, the model overestimates the level of binding at concentrations of the unlabeled ligand above 10 nM. The discrepancy arises from the [^{3}H]histamine-dependent increase in specific binding associated with the sites of low affinity (i.e., K_{A_2} when n = 2), which exceeds that predicted by scheme 2. In terms of eq. 3 (n = 2), the difference in F'_2 obtained from best fits to the data *per se* exceeds that inferred from the best fit of eq. 4. The anomalous behavior of N^{α}-methylhistamine recalls that of unlabeled histamine, where the radioligand exerts an unacceptably small or opposite effect on the observed value of F'_2. Because the disagreement persists at any value of n, the problem cannot be attributed to a degree of heterogeneity beyond the resolution of the data.

An inspection of Table 2 reveals ligand-dependent differences in the distribution of sites between the two states (F_2) and in the affinity of [^{3}H]histamine as inferred from its effect on the inhibitory behavior of the unlabeled ligand (K_{P_j}). The fitted estimates of K_{P_2} vary 1600-fold, from 4.7 nM with burimamide to 7.4 mM with N^{α}-methylhistamine. There is less variation in K_{P_1}, which differs by only 14-fold between the minimum of 0.37 nM with imidazolylpropylguanidine and the maximum of 5.1 nM with SK&F 92540; the range is only 2.3-fold if imidazolylpropylguanidine is excluded, and the mean obtained for the other 12 compounds (log $K_{P_1} = -8.49 \pm 0.04$) agrees well with the value obtained for histamine alone (log $K_{P_1} = -8.45$). If the binding patterns indeed reflect distinct and noninteracting sites, as in scheme 2, the affinities of [^{3}H]histamine and the relative distribution of sites between the two states are expected to be the same with all ligands. The differences raise the possibility that binding is not strictly competitive.

Caution is in order when comparing the fitted values of K_{P_2}, which is correlated with F_2 and $[R]_t$ at relatively low concentrations of [^{3}H]histamine (i.e., $[P] \ll K_{P_2}$). A more reliable parameter under the circumstances is the ratio $[R_2]_t/K_{P_2}$, and the mean values normalized per g of protein show a 30-fold variation among the 13 compounds tested (Table 2). If K_{P_j} is the same throughout, in accord with scheme 2, the variation in $R_{2,t}/K_{P_2}$ is a reflection of differences in capacity. A measure of the latter is provided by the quantity $B_{A=0} - B_{A\to\infty}$ (ΔB), as estimated from best fits of eq. 3 to the data from individual experiments. The results summarized in Table 2 represent 37 experiments, and the mean values of ΔB for each compound are presented relative to the mean for all compounds. The relative values of ΔB are in good agreement, and there is no relationship with the corresponding values of $R_{2,t}/K_{P_2}$. It follows that differences in the latter cannot be attributed to differences in capacity among different experiments.

Ligand-related differences in the affinity for [^{3}H]histamine and in the distribution of sites were examined further by testing pairs of ligands in simultaneous analyses with separate and common values of K_{P_1}, K_{P_2}, and F_2 (eq. 4, n = 2). The procedure was analogous to that described previously to test for differences in F'_2 (eq. 3) (see Table 4 in Ref. 1). Of the 78 possible combinations, 59 show a highly significant increase in the sum of squares when both ligands share the same values of the three parameters expected to be invariant ($p < 0.001$); the increase is moderate for 12 combinations ($0.05 > p > 0.001$) and negligible for only seven ($p > 0.05$). Discrepancies identified in this manner cannot be resolved by adding more parameters within the context of the same model. Of the 71 combinations in which the sum of squares is greater with single values of K_{P_j} and F_j for both ligands, 13 show no appreciable reduction with three classes of sites rather than two ($p > 0.05$). The decrease is significant for 58 combinations ($p < 0.05$), but the sum of squares generally remains greater than that obtained with separate values of K_{P_j} and F_j for each ligand ($p < 0.05$); the discrepancy is resolved for only 13 combinations. There is no further improvement with four classes of sites. Differences also can be demonstrated by comparisons involving the data from three or more ligands rather than only two.

The noncompetitive nature of the inhibition can be illustrated by a comparison of experimental and simulated data in the context of scheme 2. The curves presented in Fig. 5 were

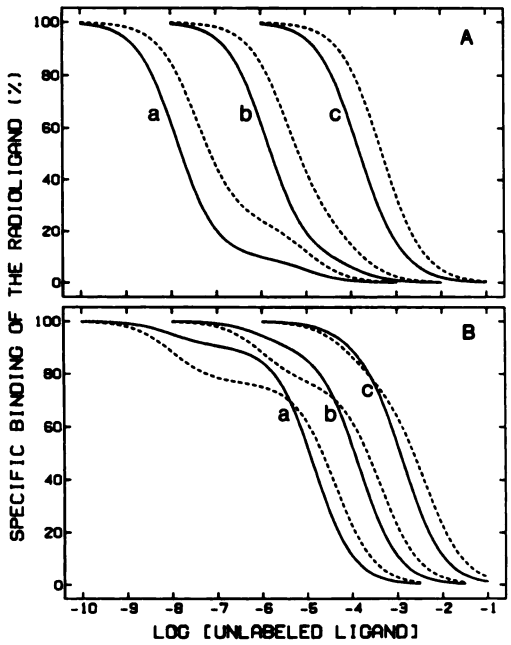

Fig. 5. Inhibition at two classes of sites differing in affinity for the probe and the unlabeled ligand. Eq. 4 ($n = 2$) was used to simulate the binding patterns expected of six hypothetical ligands at two concentrations of a radiolabeled probe (——, 1.4 nM; - - -, 11 nM); the values of K_{P_1}, K_{P_2}, and F_2 were the same throughout and were taken as those listed for histamine in Table 2 (log $K_{P_1} = -8.452$, log $K_{P_2} = -6.340$, and $F_2 = 0.9079$). The compounds represented in A show the same preference as the probe for the two classes of sites (i.e., $K_{A_2}/K_{A_1} > 1$); those in B show the opposite preference (i.e., $K_{A_1}/K_{A_2} > 1$). The individual values of K_{A_j} in A are as follows: *a*, log $K_{A_1} = -8$, log $K_{A_2} = -5$; *b*, log $K_{A_1} = -6$, log $K_{A_2} = -4$; *c*, log $K_{A_1} = -4$, log $K_{A_2} = -3$. Those in B are as follows: *a*, log $K_{A_1} = -5$, log $K_{A_2} = -8$; *b*, log $K_{A_1} = -4$, log $K_{A_2} = -6$; *c*, log $K_{A_1} = -3$, log $K_{A_2} = -4$.

computed according to eq. 4 ($n = 2$), with parameters selected to reflect the conditions of the assays represented in Table 2; inhibition is shown at two concentrations of the radioligand (1.4 nM and 11 nM), and the values of K_{P_j} and F_j were taken as those listed for histamine alone. Three of the hypothetical compounds mimic the probe in their preference for the labeled sites (i.e., $K_{A_1}/K_{A_2} < 1$), and the same preference was found for seven of the eight H_2 agonists listed in Table 2. The simulated curves in Fig. 5A resemble the binding patterns illustrated in Fig. 2A, but the agreement is only qualitative. Of the 28 pairs of agonists compared quantitatively in terms of eq. 4 ($n = 2$), 22 show significant differences in K_{P_1}, K_{P_2}, and F_2 ($p < 0.05$). A different pattern emerges with compounds that exhibit the opposite preference, relative to that of the probe (i.e., $K_{A_1}/K_{A_2} > 1$). As illustrated in Fig. 5B, the normalized binding profiles are expected to intersect when the affinity of the compound for the two classes of sites differs by about 10-fold or more. H_2 antagonists all differ from histamine in their rank order of K_{A_1} and K_{A_2} (Table 2), but only one of the five compounds tested exhibits the intersection predicted by scheme 2 (Fig. 2B). The differences in K_{P_1}, K_{P_2}, and F_2 are significant for all 10 pairs of antagonists ($p < 0.00001$).

Although scheme 2 is mechanistically inappropriate, parametric values obtained from eq. 4 reveal an empirical relationship similar to that found with eq. 3 and described in the preceding paper (see Fig. 5 in Ref. 1). As noted above, H_2 agonists and antagonists can be differentiated on the basis of their absolute preference for the labeled sites (i.e., K_{A_2}/K_{A_1} in Table 2). The sole exception to this trend is the H_2 agonist impromidine, which is also the least discriminatory of the 13 compounds tested. Of particular interest are the compounds (*R*)-(−)-sopromidine and imidazolylpropylguanidine, which are agonists at H_2 receptors but antagonists at H_3 receptors (8); all other compounds are either agonists or antagonists in both systems (1). The relative preference of histaminic ligands for the two classes of sites accounts in part for the small effect of [^{3}H]histamine on the binding of antagonists, which generally are less sensitive than agonists to an increase in the concentration of the radioligand (e.g., $IC_{50(11)}/IC_{50(1.4)}$ in Table 2).

Discussion

Low concentrations of [^{3}H]histamine have been found to label a population of G protein-linked receptors in washed membranes from guinea pig cerebral cortex (1). The time dependence and the concentration dependence of binding suggest that the labeled sites are functionally heterogeneous; association and dissociation of the radioligand are biexponential processes, and binding at equilibrium reveals Hill coefficients less than 1 for histamine and several histaminic ligands (1). For a system at thermodynamic equilibrium, the dispersion of affinities implied by Hill coefficients less than 1 could arise in at least three ways, as follows: first, two or more classes of distinct, noninterconverting, and mutually independent sites may differ in their affinity for the ligand (i.e., scheme 2 in Ref. 1); second, intrinsically identical sites may exist in two or more interconverting states arising from transient association with other, stoichiometrically limiting proteins within the membrane (e.g., the mobile receptor model); and third, successive equivalents of the ligand may bind to interacting sites in a cooperative manner. The ambiguity of the data precludes a mechanistic interpretation of the binding patterns and thereby complicates the pharmacological identification of the labeled sites.

Ligand-dependent differences in the apparent distribution of sites inferred from eq. 3 argue against the notion of intrinsic heterogeneity, but the results are not definitive. All of the data were acquired at a single concentration of [^{3}H]histamine, and discrepancies among different ligands can be rationalized by assuming a degree of heterogeneity beyond the resolution of the data. This option is ruled out in the present report, where the categorical rejection of scheme 2 is made possible by the implicit use of [^{3}H]histamine as an internal control; when binding of the unlabeled ligand is characterized at more than one concentration of the radiolabeled probe, the binding properties of the latter can be inferred from its effect on the inhibitory behavior of the former (e.g., Fig. 3, *inset*). Such an approach requires at least two concentrations of the probe, and discrepancies between the model and the present data tend to emerge only from comparisons among different unlabeled ligands; in most cases, the model is in good agreement with the combined data on individual ligands (Fig. 2). One exception to this pattern occurs with the agonist N^{α}-methylhistamine, where the model is unable to account for the binding patterns obtained at even two concentrations of [^{3}H]histamine. A second exception is histamine itself, partly because data acquired by isotopic dilution require fewer parameters; in the case of scheme 2, the model is fully defined when inhibition by unlabeled histamine is characterized at a single concentration of the radioligand.

The failure of scheme 2 lies in parametric values that appear

to reflect noncompetitive interactions between [^{3}H]histamine and the unlabeled ligand. Binding nevertheless is mutually exclusive, in that saturating concentrations of all ligands were found to inhibit binding to the same absolute level at either concentration of [^{3}H]histamine. The apparently noncompetitive effects therefore seem likely to arise from intrinsically competitive binding, a situation that can occur with either of the alternatives to scheme 2 listed above. The mobile receptor model is both qualitatively attractive and difficult to test, but it nevertheless appears to be inappropriate on several counts. In contrast, observations that are at variance with scheme 2 and the mobile receptor model can be accommodated in terms of cooperative effects. The ability to distinguish among alternative hypotheses is due in part to the unorthodox behavior of histaminic antagonists.

Mobile receptor model. The prevailing view of G protein-mediated transduction is based on the notion of a transient complex between the receptor and the G protein. Similarly, the dispersion of affinities identified in binding studies is commonly attributed to a ligand-regulated mixture of free and G protein-coupled receptors (2, 9). Quantitative descriptions of the latter have been formulated in terms of the mobile receptor hypothesis of Jacobs and Cuatrecasas (10) and similar proposals by other investigators (11, 12). The simplest variant involves a spontaneous equilibrium within the membrane between free receptor (R) and free G protein (G) on the one hand and a heterodimeric complex (RG) on the other (13); agonists are thought to bind with higher affinity to RG than to R and thereby to stabilize the RG complex, whereas antagonists either are indifferent or exhibit the opposite preference. Opposing effects of agonists and antagonists on the equilibrium between R and RG can appear to be noncompetitive when the data are evaluated in terms of distinct and independent sites.

Explicit applications of the mobile receptor model are few, but it has been reported to describe the binding of agonists to α_2-adrenergic receptors (14, 15), β-adrenergic receptors (13), M_2 muscarinic receptors (16–18), D_2 dopaminergic receptors (19), and A_1 adenosine receptors (20). Ehlert (17) and Ehlert and Rathbun (18) concluded that the model describes the binding properties of cardiac muscarinic receptors provided that there are fewer G proteins than receptors in the interacting pools. Minton and Sokolovsky (16) found that binding to M_2 receptors cannot be described by the model if the pool of G proteins is homogeneous, but the discrepancy is resolved if two distinct G proteins compete for the relevant site on the receptor. Similarly, Leung *et al.* (20) found that either two classes of G protein or two classes of receptor are required for agreement between the model and binding properties of A_1 adenosine receptors. Neubig *et al.* (15) have suggested that about one third of α_2 receptors are functionally inaccessible to a G protein. In most reports, the effect of guanyl nucleotides has been rationalized as an irreversible loss of G proteins (13, 15, 16, 19).

Despite widespread acceptance of mechanistic proposals based on the notion of a transient complex, binding is analyzed almost universally in terms of scheme 2. This practice is questionable if G proteins indeed exchange at a site on the receptor (6), and apparently noncompetitive binding is an artifact arising from differences between one model and the other. The effect is illustrated by the parametric values listed in Table 3, which are derived from best fits of eq. 4 to data simulated according to the mobile receptor model. The latter presupposed a radiolabeled probe (P), such as [^{3}H]histamine, with higher affinity for RG (K_{PG}) than for R (K_P) (i.e., $K_P/K_{PG} = 10^4$) and a series of 11 unlabeled ligands (A) with the same or opposite preference relative to that of the probe (i.e., $K_A/K_{AG} = 10^5$ to 10^{-5}). When analyzed in terms of scheme 2, the simulated data yield values of K_{A_j} and K_{P_j} that lie within a range established by K_{AG} or K_{PG} on the one hand and by K_A or K_P on the other (Table 3). Accordingly, the absolute value of log (K_A/K_{AG}) or log (K_P/K_{PG}) exceeds that of log (K_{A_2}/K_{A_1}) or log (K_{P_2}/K_{P_1}), respectively. Because the values of K_{P_j} and F_2 obtained from eq. 4 depend upon the unlabeled ligand (Table 3), the model predicts apparently noncompetitive behavior similar to that observed at the sites labeled by [^{3}H]histamine (Table 2).

Simulations with the mobile receptor model were performed with parametric values at which the RG complex comprises 50% of the receptors; the level of coupling increases to 61% at the lower concentration of the probe and to 81% at the higher concentration. The conditions were chosen to mimic the unusual observation that the dispersion of affinities at the sites labeled by 1.4 nM [^{3}H]histamine can be of comparable breadth for agonists ($n_H \geq 0.78$) and antagonists ($n_H \geq 0.66$) (1). Values of F'_2 varied over a broad range (1), implying that the dispersion derives primarily from ligand-dependent changes in the degree of coupling (6). G protein-linked receptors typically appear homogeneous with respect to antagonists ($n_H = 1$) and heterogeneous with respect to agonists ($n_H < 1$). In terms of the mobile receptor model, this behavior implies an equilibrium that lies predominantly toward uncoupled receptor in the absence of ligands (e.g., Ref. 13). Agonists must favor RG over R if the system is to perform as advertised, but the effect of antagonists is unclear; there may be a preference for R over RG, or the ligand may not distinguish between the two forms. This question is partially resolved in some systems, where the sites exhibit limited heterogeneity toward antagonists, and guanyl nucleotides promote an interconversion to the state of higher affinity (e.g., Refs. 19 and 21). Antagonists therefore seem to favor R over RG, although the full extent of the difference in affinity is difficult to assess. Precoupling has been estimated at 40% for the D_2 dopaminergic receptor (19) and as high as 85% for the A_1 adenosine receptor (20), which resembles the present system in some respects.

With appreciable levels of precoupled receptor, a radiolabeled antagonist that favors R over RG is expected to show a substantial increase in specific binding upon dissociation of the RG complex by the addition of GMP-PNP. The H_2 antagonists [^{3}H]tiotidine and [^{125}I]iodoaminopotentidine label H_2 receptors in homogenates of guinea pig cortex (22, 23), but neither compound has been reported to be sensitive to guanyl nucleotides. Even the effect on the inhibitory behavior of histamine appears to be small (23). As illustrated in Fig. 6, GMP-PNP is without effect on the binding of [^{3}H]tiotidine to membranes prepared according to the procedures used in the present investigation. Two classes of sites are required in terms of eq. 4, and the fitted values of K_{P_1} and $R_{1,t}$ compare favorably with the estimates of affinity and capacity reported previously (22). Both $R_{1,t}$ and its contribution to specific binding are comparable in magnitude to the corresponding values obtained for [^{3}H]histamine, and any interconversion from one state to the other ought to be readily discernible. If guanyl nucleotides indeed destabilize RG (2), the lack of sensitivity to GMP-PNP suggests

TABLE 3

Behavior of the mobile receptor model when the probe and unlabeled ligand exhibit the same or opposite preferences for uncoupled and G protein-coupled receptors

Hypothetical binding curves were simulated according to the mobile receptor model formulated as described previously (eqs. 2 and 3 in Ref. 6; eqs. 106 and 107 in Ref. 7). The parameters K_A and K_{AG} represent the equilibrium dissociation constants for binding of the unlabeled ligand (A) to the free receptor (R) and the receptor-G protein complex (RG), respectively (i.e., K_A = [A][R]/[AR] and K_{AG} = [A][RG]/[ARG]); K_P and K_{PG} are the corresponding constants for the radiolabeled probe (P). The parameter K_G represents the equilibrium dissociation constant for the interaction between R and G (i.e., K_G = [R][G]/[RG]). Parametric values common to all simulations were as follows: log K_P = −5, log K_{PG} = −9, log K_A = −6, log K_G = −10.301, $[R]_t$ = 100 pM, $[G]_t$ = 100 pM, and NS = 0.005; log K_{AG} was assigned different values as shown in the table. To mimic the apparent behavior of the sites labeled by [^{3}H]histamine, the values of $[R]_t$, $[G]_t$, and K_G were selected to achieve 50% precoupling of R and G in the absence of P or A (i.e., [RG]/$[R]_t$ = 0.5). A total of 200 data points were calculated at two values of log [P] (−9 and −8) and equal increments of log [A] over a range sufficient to reduce specific binding from at least 99.9% to <0.1% of the maximal value. Eq. 4 (n = 2) was fitted to the simulated data to obtain the values of K_{A_1}, K_{P_1}, and F_2 listed in the table; the fitted values of $[R]_t$ range from 93.7 pM when log K_{AG} = −11 to 89.3 pM when log K_{AG} = −1, and NS is essentially 0.005 throughout. Estimates of n_H were obtained from best fits of eq. 1, with $B_{A=0}$ and $B_{A=\infty}$ fixed at the asymptotic values of the simulated curves (1 nM P, $B_{A=0}$ = 35.48 pM, $B_{A=\infty}$ = 5 pM; 10 nM P, $B_{A=0}$ = 123.5 pM, $B_{A=\infty}$ = 50 pM). All points were weighted equally throughout. The variables [P] and [A] represent free concentrations in the model used for the simulations and in the expression used to calculate $[P]_b$ in the analyses with eq. 4.

Mobile receptor model		Eq. 4 (n = 2)							Eq. 2	
−log K_{AG}	K_A/K_{AG}	−log K_{A_1}	−log K_{A_2}	−log K_{P_1}	−log K_{P_2}	F_2	K_{A_2}/K_{A_1}	K_{P_2}/K_{P_1}	n_H at 1 nM P	n_H at 10 nM P
11	100,000	10.81	9.90	8.80	7.96	0.21	8.0	6.9	0.975	0.988
10	10,000	9.81	8.90	8.80	7.96	0.21	8.0	6.9	0.975	0.988
9	1,000	8.81	7.92	8.80	7.97	0.21	7.8	6.8	0.975	0.989
8	100	7.82	7.01	8.81	8.02	0.22	6.4	6.3	0.977	0.993
7	10	6.86	6.35	8.84	8.13	0.28	3.2	5.1	0.990	1.000
6	1	6.00	6.01	8.85	8.21	0.29	0.97	4.4	0.996	0.958
5	0.1	5.49	5.91	8.88	8.39	0.40	0.39	3.1	0.947	0.870
4	0.01	5.36	5.87	8.89	8.44	0.44	0.31	2.8	0.922	0.841
3	0.001	5.34	5.87	8.89	8.44	0.45	0.30	2.8	0.919	0.837
2	0.0001	5.34	5.87	8.89	8.45	0.45	0.29	2.8	0.918	0.837
1	0.00001	5.34	5.87	8.89	8.45	0.45	0.29	2.8	0.918	0.837

that [^{3}H]histamine and [^{3}H]tiotidine do not label the G-coupled and uncoupled forms of the same receptor.

Noncompetitive effects found in the binding studies with [^{3}H]histamine resemble those predicted by the mobile receptor model (see Tables 2 and 3), but preliminary analyses failed to deliver a satisfactory fit when the data were analyzed explicitly in terms of the model described previously and in Table 3 (i.e., eqs. 108–111 in Ref. 7). The problem lies partly in the breadth of the binding patterns, reflected in the low values of n_H, and in the assumption that the populations of receptors and G proteins were homogeneous. As demonstrated by Lee *et al.* (6), the nature of the mobile receptor model tends to restrict parameter space when data from such systems are analyzed in terms of the Hill equation or scheme 2. With the hypothetical compounds listed in Table 3, for example, the value of K_A/K_{AG} in the mobile receptor model was varied from 10^5 to 10^{-5}; in contrast, the range for corresponding values of K_{A_2}/K_{A_1} is from 8.0 to 0.29. These and related constraints preclude a mechanistically consistent description of the data with comparatively simple formulations of the model.

The limitations described above can be relaxed or avoided if the model is expanded to encompass the potential complexity of native membranes. Multiple G proteins may compete for the same site on the receptor or vice versa (16, 20). Also, different subtypes of receptor and their corresponding G proteins may coexist independently, perhaps localized in different regions of the membrane. It seems likely that the additional flexibility gained by such refinements would resolve many of the problems encountered when fitting relatively naive versions of the model. The number of possibilities is large, however, owing in part to the lack of biochemical data on the proteins involved; also, any such scheme would involve a large number of parameters, many of which would be undefined with the data presently available. More suitable data may be difficult to obtain pending the development of radioligands with high affinity for those sites

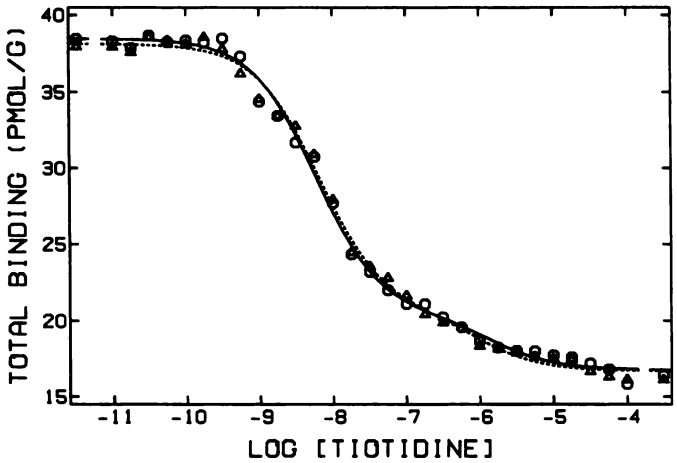

Fig. 6. Isotopic dilution of [^{3}H]tiotidine. Total binding was measured after incubation of the membranes (1.44 mg of protein/ml) with [^{3}H]tiotidine (2.51 nM) plus the unlabeled analogue at the concentrations shown on the *abscissa*; parallel assays were performed in the absence of guanyl nucleotide (○) and in the presence of 0.1 mM GMP-PNP (△). Binding was assayed in a sample volume of 250 μl, and the reaction was terminated by filtration after equilibration for 4 hr at 20°; conditions otherwise were as described in Materials and Methods in the preceding paper (1). The *lines* represent best fits of eq. 4 (n = 2) to the data. Parametric values are as follows: without GMP-PNP (○, ——), log K_{P_1} = −8.49 ± 0.08, log K_{P_2} = −5.84 ± 0.18, F_2 = 0.98 ± 0.01, $R_{1,t}$ = 42 ± 17 pmol/g of protein, $R_{2,t}$ = 2170 ± 880 pmol/g of protein, and NS = 0.0096 ± 0.0001; with GMP-PNP (△, – – –), log K_{P_1} = −8.41 ± 0.08, log K_{P_2} = −6.02 ± 0.18, F_2 = 0.97 ± 0.01, $R_{1,t}$ = 45 ± 16 pmol/g of protein, $R_{2,t}$ = 1560 ± 600 pmol/g of protein, and NS = 0.0096 ± 0.0001. There is no significant increase in the weighted sum of squares if the analysis is repeated with single values of all parameters for the two sets of data (p = 0.42). *Points at the lower end of the abscissa* represent total binding in the absence of unlabeled tiotidine; *points at the upper end* represent total binding in the presence of 1.0 mM unlabeled histamine and were omitted from the analysis.

that cannot be measured at practicable concentrations of [^{3}H] histamine.

The potential complexity of the mobile receptor model notwithstanding, it may be inappropriate to resolve the problem simply by adding parameters within the same mechanistic context. The Hill coefficient exceeds 1 for the inhibitory effect of pyridylethylamine, SK&F 93479, and possibly (*R*)-α-methylhistamine at the sites labeled by [^{3}H]histamine (Table 3 in Ref. 1). An artifact is unlikely (7); the system seems to be at equilibrium, and no depletion of the unlabeled ligand is expected at the concentrations that cause inhibition (>1 μM). High values of n_H therefore appear to reflect the mechanism of binding and may share a common origin with the lower values found with most compounds. There is an upper limit of 1 on the Hill coefficient obtainable with scheme 2 or the mobile receptor model, regardless of the number of receptors or G proteins postulated for the latter.

Several observations appear to contradict a basic assumption of the mobile receptor model and related schemes, namely, that receptors and G proteins exchange randomly between coupled and uncoupled forms. The model predicts that estimates of K_{A_j} or K_{P_j} obtained in terms of scheme 2 (eq. 4) will be highly sensitive to the affinity of the receptor for the G protein (K_G) and to the local concentrations of R and G within the membrane (6). In contrast, the apparent affinities of histamine and 19 other ligands are similar or the same for the labeled sites in cortical membranes from guinea pig and in the digitonin-solubilized preparation from rat (Fig. 6D in Ref. 1). Solubilization presumably effects a 1000-fold decrease in the overall concentrations of R and G if dissociation is spontaneous, and the receptor also may gain access to G proteins that are inaccessible in the native membrane. The effective volume may be restricted somewhat if the proteins are embedded in micelles or vesicles, but the randomization that presumably accompanies disruption of the membrane can be expected to reduce local concentrations from those in the native state. It seems unlikely that virtually identical values of K_{P_j} and K_{A_j} could be obtained before and after solubilization if those parameters reflected concentration-dependent interactions between receptor and G protein. Furthermore, the effects of GMP-PNP and magnesium on the binding of histamine in solubilized preparations are reversible (24); an interconversion from high to low affinity is expected to be irreversible in solution if the low affinity sites arise from the physical separation and subsequent diffusion of the G protein from the receptor.

A more basic snag emerges from the trends illustrated in Fig. 5 of the preceding report (1), where the binding patterns have been examined empirically in terms of eq. 3. A negative correlation between log (K_2/K_1) and F'_2 suggests that agonists increase the propensity of the sites to adopt the state of higher affinity for the ligand; in contrast, antagonists reveal a positive correlation and therefore appear to favor the state of lower affinity. The latter observation leads to a paradox if the ligand is believed to act by perturbing a pre-existing equilibrium between the two states; it implies a violation of microscopic reversibility and suggests that any such scheme is inappropriate.

The expected behavior of the mobile receptor model is illustrated in Fig. 7, where the parametric values represent best fits of eq. 3 (n = 2) to simulated data. The simulations were performed as described in the legend to Table 3, except that a

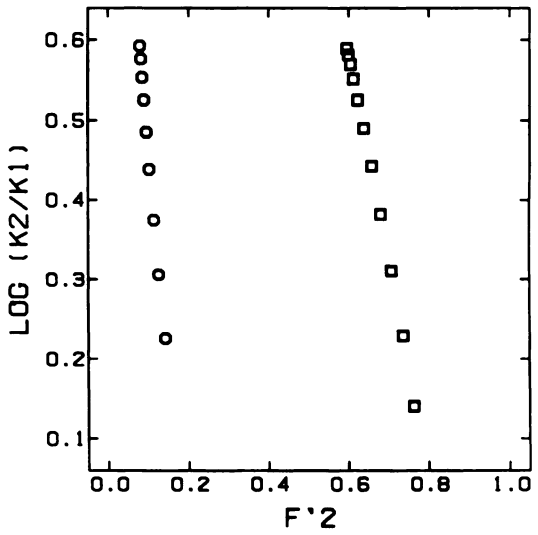

Fig. 7. Relationship between relative potency and the apparent distribution of sites in binding patterns computed according to the mobile receptor model. Data for 20 hypothetical ligands were simulated at a single concentration of the probe (log [P] = −9); the values of K_{AG} are listed below, and other conditions were as described in the legend to Table 3. Values of log (K_2/K_1) and F'_2 plotted in the figure are from the best fits of eq. 3 (n = 2) to the simulated data ($K_2 > K_1$); $B_{A=0}$ and $B_{A=\infty}$ were fixed as described in the legend to Table 3 for the analyses according to eq. 2. Different symbols denote the preference of the ligand for the uncoupled receptor (□, $K_{AG}/K_A > 1$) or the receptor-G protein complex (○, $K_{AG}/K_A < 1$). The value of log K_A was −6 throughout (Table 3); the value of log K_{AG} was incremented by 0.2 log unit from −8.4 to −6.8 (○, *top* to *bottom*) or from −6.0 to −4.0 (□, *bottom* to *top*). Individual estimates of log K_1, log K_2, and F'_2 (eq. 3) are as follows: when $K_{AG}/K_A <$ 1 (○), −8.01, −7.41, 0.0795; −7.81, −7.23, 0.0816; −7.61, −7.05, 0.0848; −7.41, −6.89, 0.0890; −7.21, −6.73, 0.0949; −7.02, −6.58, 0.102; −6.82, −6.45, 0.113; −6.63, −6.33, 0.126; −6.45, −6.22, 0.141; when $K_{AG}/K_A > 1$ (□), −5.90, −5.76, 0.764; −5.84, −5.61, 0.735; −5.79, −5.48, 0.707; −5.75, −5.37, 0.680; −5.72, −5.27, 0.657; −5.69, −5.20, 0.638; −5.67, −5.15, 0.623; −5.66, −5.11, 0.612; −5.65, −5.08, 0.604; −5.64, −5.06, 0.599; −5.64, −5.05, 0.404.

narrower range of K_A/K_{AG} was selected for the hypothetical ligands. As pointed out previously (6), there is an inverse relationship between the difference in apparent affinity for the two classes of sites [i.e., log (K_2/K_1)] and the number of sites apparently in the state of lower affinity (F'_2). That relationship is observed irrespective of whether the unlabeled ligand and the probe exhibit the same or the opposite preference for the two states, although the range of values obtained for F'_2 is different in each case. The relationships in Fig. 7 reflect the propensity of all ligands to increase the number of sites in the state of higher affinity, that is, free R when K_{AG} exceeds K_A, and the RG complex when K_A exceeds K_{AG}. A comparison of Fig. 7 with Fig. 5 in the preceding paper (1) illustrates the anomalous behavior of antagonists at the sites labeled by [^{3}H] histamine.

Cooperativity. G proteins linked to muscarinic receptors exhibit multiple states of affinity for guanyl nucleotides (e.g., Refs. 25 and 26), and the apparent heterogeneity appears to derive from cooperative effects in the binding of successive equivalents of ligand (26). Carbachol promotes an apparent interconversion of sites from higher to lower affinity for GDP, and the effect emerges as a change in the degree of cooperativity between one equivalent of nucleotide and the next (26). The agonist-sensitive binding of GDP to G proteins mimics the guanyl nucleotide-sensitive binding of agonists to muscarinic

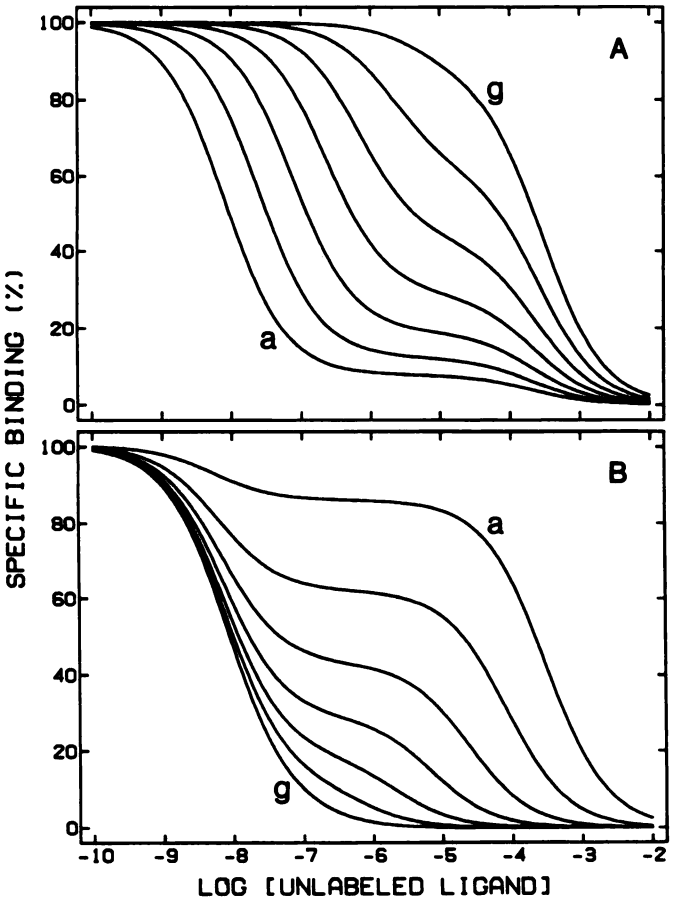

Fig. 8. Cooperative binding to a bivalent receptor. The inhibitory effects of 14 unlabeled ligands on the specific binding of a probe were simulated as described in the legend to Table 4.

receptors. In view of the symmetrical nature of the system, cooperativity at the G protein implies that a similar phenomenon underlies binding to the receptor.

For the sites labeled by [^{3}H]histamine, models that permit cooperative interactions can account for most if not all of the effects that are anomalous in terms of scheme 2 or the mobile receptor model. Hill coefficients greater than 1 imply positive cooperativity between successive equivalents of the unlabeled ligand, and it follows by analogy that Hill coefficients less than 1 may reflect negative cooperativity. Ligand-dependent differences in the apparent distribution of sites between states (i.e., F'_2 in eq. 3) and the curious tendency of histaminic antagonists to favor the state of lower affinity both can be attributed to differences in the degree of cooperativity between one equivalent of ligand and the next. The presumed oligomer that accounts for the binding properties does not dissociate into free subunits, at least under the conditions of the experiments, and the relative concentrations of the interacting proteins will not appear in explicit formulations of the model; such schemes therefore can account for retention of the native properties upon dissolution of the membrane.

The versatility of cooperative systems is illustrated in Fig. 8, where the lines have been simulated according to a scheme in which two ligands compete for a bivalent receptor (7, 26, 27). The parametric values used in the simulation are listed in Table 4 together with the values of log (K_2/K_1) and F'_2 for the equivalent curves in terms of eq. 3. Ligand-dependent differences in F'_2 arise from differences in the degree of cooperativity between the unlabeled ligand and the probe. The quantity K_2/K_1 is determined by the degree of cooperativity between successive equivalents of the unlabeled ligand. Because the two cooperative effects are independent, there is no restriction on the relationship between log (K_2/K_1) and F'_2. As illustrated in Fig. 8 and Table 4, a series of ligands can appear to favor the state of high affinity (Fig. 8A and Table 4A) or low affinity (Fig. 8B and Table 4B) when binding is assessed in terms of a sum of hyperbolic terms. The model therefore can account for the trends illustrated in Fig. 5 of the preceding paper (1) and found previously in the binding of agonists to β-adrenergic receptors (5, 6), although it is silent on the underlying cause.

TABLE 4

Behavior of a bivalent receptor exhibiting cooperative effects

Hypothetical binding curves were simulated according to a model for a bivalent cooperative receptor, formulated as described previously (eq. 4 in Ref. 26; eqs. 166–170 in Ref. 7). The microscopic dissociation constants for binding of the probe (P) and the unlabeled ligand (A) to the equivalent sites of a vacant receptor are shown below as K_P and K_A. The parameters *a*, *b*, and *c* represent the cooperativity factors for the change in affinity at the second site upon occupancy of the first; *a* and *b* refer to the effect with two equivalents of P or A, respectively, and *c* refers to that with one equivalent of each. Further details are described in Refs. 7 and 26. In all stimulations, the values of log K_P and log *a* were taken as −8.5 and 2.0, respectively; [P] was set at 1 nM, and the values of log *b* and log *c* are listed in the table. In A, log K_A was incremented by 0.5 log unit from −8.0 (curve a) to −5.0 (curve g). In B, log K_A was taken as −8.0 throughout. Eq. 3 ($n = 3$) was fitted to the data to obtain the values of K_1, K_2, and F'_2 represented in the table. The simulated curves are illustrated in Fig. 8.

	Curve	Bivalent receptor		Eq. 3 ($n = 2$)	
		log *b*	log *c*	log (K_2/K_1)	F'_2
A	a	4.0	−1.0	4.42	0.08
	b	3.5	−0.8	3.93	0.12
	c	3.0	−0.6	3.45	0.19
	d	2.5	−0.4	2.99	0.29
	e	2.0	−0.2	2.54	0.43
	f	1.5	0	2.12	0.62
	g	1.0	0.2	1.72	0.87
B	a	4.0	0.2	4.74	0.86
	b	3.5	0	4.13	0.62
	c	3.0	−0.2	3.55	0.43
	d	2.5	−0.4	2.99	0.29
	e	2.0	−0.6	2.45	0.19
	f	1.5	−0.8	1.92	0.11
	g	1.0	−1.0	1.38	0.04

The compounds presented here and in the accompanying report (1) reveal up to two classes of sites in terms of eq. 3, and a bivalent receptor or a dimer is the simplest cooperative system that can be envisaged. The model examined in Table 4 and Fig. 8 can be used to describe the present data on the inhibitory effect of various ligands at 1.4 nM and 11 nM [^{3}H]histamine, and there is good agreement among parametric values unique to [^{3}H]histamine (i.e., K_P and *a* in Table 4); discrepancies analogous to those presented in Table 2 are largely avoided, and the data for different ligands can be pooled with relatively little effect on the goodness of fit.[1] The marked improvement obtained with a comparatively frugal model suggests that it may be useful to consider cooperativity as an alternative to the mobile receptor model and related schemes. Similar effects may account for the binding properties of other G protein-linked receptors, because it seems unlikely that those labeled by [^{3}H] histamine are mechanistically unique.

[1] Preliminary results have been presented elsewhere (28).

References

1. Sinkins, W. G., M. Kandel, S. I. Kandel, W. Schunack, and J. W. Wells. G protein-linked receptors labeled by [^{3}H]histamine in guinea pig cerebral cortex. I. Pharmacological characterization. *Mol. Pharmacol.* **43**:569–582 (1993).
2. Birnbaumer, L., J. Abramowitz, and A. M. Brown. Receptor-effector coupling by G proteins. *Biochim. Biophys. Acta* **1031**:163–224 (1990).
3. Waelbroeck, M., P. Robberecht, P. Chatelain, and J. Christophe. Rat cardiac muscarinic receptors. I. Effects of guanine nucleotides on high- and low-affinity binding sites. *Mol. Pharmacol.* **21**:581–588 (1982).
4. Birsdall, N. J. M., A. S. V. Burgen, and E. C. Hulme. The binding of agonists to brain muscarinic receptors. *Mol. Pharmacol.* **14**:723–736 (1978).
5. Kent, R. S., A. De Lean, and R. J. Lefkowitz. A quantitative analysis of *beta*-adrenergic receptor interactions: resolution of high and low affinity states of the receptor by computer modeling of ligand binding data. *Mol. Pharmacol.* **17**:14–23 (1980).
6. Lee, T. W. T., M. J. Sole, and J. W. Wells. Assessment of a ternary model for the binding of agonists to neurohumoral receptors. *Biochemistry* **25**:7009–7020 (1986).
7. Wells, J. W. Analysis and interpretation of binding at equilibrium, in *Receptor-Ligand Interactions. A Practical Approach* (E. C. Hulme, ed.). Oxford University Press, Oxford, UK, 289–395 (1992).
8. Arrang, J. M., M. Garbarg, and J.-C. Schwartz. Histamine synthesis and release in CNS: control by autoreceptors (H_3). *Adv. Biosci.* **51**:143–153 (1985).
9. Casey, P. J., and A. G. Gilman. G protein involvement in receptor-effector coupling. *J. Biol. Chem.* **263**:2577–2580 (1988).
10. Jacobs, S., and P. Cuatrecasas. The mobile receptor hypothesis and "cooperativity" of hormone binding: application to insulin. *Biochim. Biophys. Acta* **433**:482–495 (1976).
11. Boeynaems, J. W., and J. E. Dumont. Quantitative analysis of the binding of ligands to their receptors. *J. Cyclic Nucleotide Res.* **1**:123–142 (1975).
12. De Haen, C. The non-stoichiometric floating receptor model for hormone sensitive adenylyl cyclase. *J. Theor. Biol.* **58**:383–400 (1976).
13. De Lean, A., J. M. Stadel, and R. J. Lefkowitz. A ternary complex model explains the agonist-specific binding properties of the adenylate cyclase-coupled β-adrenergic receptor. *J. Biol. Chem.* **255**:7108–7117 (1980).
14. Neubig, R. R., R. D. Gantzos, and R. S. Brasier. Agonist and antagonist binding to α_2-adrenergic receptors in purified membranes from human platelets. *Mol. Pharmacol.* **28**:475–486 (1985).
15. Neubig, R. R., R. D. Gantzos, and W. J. Thomsen. Mechanism of agonist and antagonist binding to α_2 adrenergic receptors: evidence for a precoupled receptor-guanine nucleotide protein complex. *Biochemistry* **27**:2374–2384 (1988).
16. Minton, A. P., and M. Sokolovsky. A model for the interaction of muscarinic receptors, agonists, and two distinct effector substances. *Biochemistry* **29**:1586–1593 (1990).
17. Ehlert, F. J. The relationship between muscarinic receptor occupancy and adenylate cyclase inhibition in the rabbit myocardium. *Mol. Pharmacol.* **28**:410–421 (1985).
18. Ehlert, F. J., and B. E. Rathbun. Signaling through the muscarinic receptor-adenylate cyclase system of the heart is buffered against GTP over a range of concentrations. *Mol. Pharmacol.* **38**:148–158 (1990).
19. Wreggett, K. A., and A. De Lean. The ternary complex model: its properties and application to ligand interactions with the D_2-dopamine receptor of the anterior pituitary gland. *Mol. Pharmacol.* **26**:214–227 (1984).
20. Leung, E., K. A. Jacobson, and R. D. Green. Analysis of agonist-antagonist interactions of A_1 adenosine receptors. *Mol. Pharmacol.* **38**:72–83 (1990).
21. Burgisser, E., A. De Lean, and R. J. Lefkowitz. Reciprocal modulation of agonist and antagonist binding to muscarinic cholinergic receptor by guanine nucleotide. *Proc. Natl. Acad. Sci. USA* **79**:1732–1736 (1982).
22. Gajtkowski, G. A., D. B. Norris, T. J. Rising, and T. P. Wood. Specific binding of [^{3}H]tiotidine to histamine H_2 receptors in guinea-pig cerebral cortex. *Nature (Lond.)* **304**:65–67 (1983).
23. Ruat, M., E. Traiffort, M. L. Bouthenet, J.-C. Schwartz, J. Hirschfeld, A. Buschauer, and W. Schunack. Reversible and irreversible labeling and autoradiographic localization of the cerebral histamine H_2 receptor using [^{125}I] iodinated probes. *Proc. Natl. Acad. Sci. USA* **87**:1658–1662 (1990).
24. Wells, J. W., and D. L. Cybulsky. Reversible interconversion among states of putative H_2 receptors in solution. *Eur. J. Pharmacol.* **183**:1731–1732 (1990).
25. Tota, M. R., K. R. Kahler, and M. I. Schimerlik. Reconstitution of the purified porcine atrial muscarinic acetylcholine receptor with purified porcine atrial inhibitory guanine nucleotide binding protein. *Biochemistry* **26**:8175–8182 (1987).
26. Chidiac, P., and J. W. Wells. Effects of adenyl nucleotides and carbachol on cooperative interactions among G proteins. *Biochemistry* **31**:10908–10921 (1992).
27. Mattera, R., B. J. R. Pitts, M. L. Entman, and L. Birnbaumer. Guanine nucleotide regulation of a mammalian myocardial muscarinic receptor system: evidence for homo- and heterotropic cooperativity in ligand binding analyzed by computer-assisted curve fitting. *J. Biol. Chem.* **260**:7410–7421 (1985).
28. Sinkins, W. G., and J. W. Wells. Apparently cooperative binding to G protein-linked receptors labeled by [^{3}H]histamine. *Soc. Neurosci. Abstr.* **18**:467 (1992).

Send reprint requests to: James W. Wells, Faculty of Pharmacy, University of Toronto, 19 Russell Street, Toronto, Ontario, Canada M5S 2S2.